QUALITY CONTROL OF WATERFLOODS ON HETEROGENEOUS CORE SAMPLES USING COMPUTER TOMOGRAPHY

Helga Baardsen, Victor Nilsen and Arvid O. Hove
STATOIL, P.O. Box 300, N-4001 Stavanger, Norway

Abstract This paper presents X-ray Computer Tomographic (CT) visualizations of water- and oilfloods performed on a heterogeneous reservoir sandstone sample. The CT-images show more or less pronounced capillary end-effects, and a layered structure in the sample is clearly shown by a miscible displacement. The porosity distribution and permeability to water for each layer are quantified.

The value of initial water saturation, S_{wi}, is strongly dependent on the method used to establish S_{wi}. The oil is produced mainly from the more permeable zone of the sample, and the residual oil saturation, S_{or}, is independent on the S_{wi}-value. The effect of rate on S_{or} is also studied.

Additional characterization of the sample was obtained by oil/water capillary pressure curve, mercury injection data, thin section and SEM analyses.

Wettability tests on parallel samples indicate a near neutral wetting characteristics. The sample became water wet after firing.

INTRODUCTION

Displacement tests on cores from a specific zone in a North Sea reservoir have indicated relatively high initial water and residual oil saturations and also a "non-traditional" shape of the water/oil relative permeability curves, as illustrated in figure 1. Most of the samples were heterogeneous, often containing coarse grains, and a typical trend for this reservoir zone is low porosity and high

permeability. To control the quality of these displacement data (input data for a simulation model), a new sample from this heterogeneous zone was selected. X-ray CT was used to describe the sample and the floods in detail.

This paper emphasizes the necessity of using a visualization technique to evaluate displacement tests on heterogeneous samples. Results from water- and oilfloods are presented.

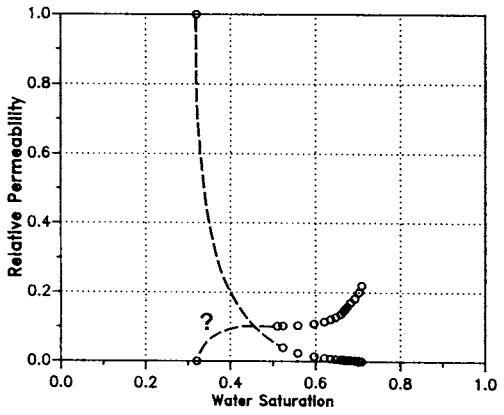

FIGURE 1 A typical rel. perm. curve for this reservoir zone.

EXPERIMENTAL

Core Material and Fluids

The sample used in the experiments is longitudinally layered and the permeability variations, based on CT-estimations, ranges from 1 to 3 Darcy. Other petrophysical properties are listed in table 1. The sample was renamed after reducing the corelength (1A) and after firing (1B). The thin section analysis reports 66% quartz, 10% K-feldspar, 4% kaolinite and 20% macro-porosity of sample 1.

Mercury injection data measured on sample 1 (using a Carlo Erba instrument), indicate pore radii in the range of 5 - 50 μm, which is 10-20 times less than estimated from thin section analyses. In the Hg-injection apparatus the pores with pore-throats larger than about 40 μm will be filled spontaneously with mercury, i.e. before data collection. This will seriously affect the measurements on coarse grained samples.

Synthetic formation chloride-brine with total dissolved solids of 20 g/kg and a refined light oil (1.27 mPas) were used. Density and viscosity of water were 1.02 g/ml and 1.03 mPas respectively. To

enhance the contrast between the fluids in the CT-studies, 100 g/kg sodium iodide was added. Density and viscosity of the iodide-water were 1.08 g/ml and 1.06 mPas respectively. In some floods viscous oil (36 mPas) was used to establish a low S_{wi}. Adding NaI to the brine did not alter the interfacial tension (water/oil) , so it was assumed that the fluids will not affect the wettability of the samples.

TABLE 1 Petrophysical properties.

	Sample 1	*Sample 1A*	*Sample 1B*
Length (cm)	8.50	4.70	4.70
Diameter (cm)	3.74	3.74	3.74
Porevolume (ml)	17.0	9.18	9.97
Porosity (%)	18.2	18.2	19.8
Grain density (g/ml)	2.64	2.64	2.64
Gas permeability (mD)	—[a]	2720	3990
Klinkenberg perm. (mD)	—[a]	2680	3900
Water permeability (mD)	1752	2320	2520

[a] Gas permeability (at $1/P_m = 1.0$) and Klinkenberg permeability (at $1/P_m = 0.0$) were not measured due to exp. limitaions.

Apparatus

The sample was mounted in a Hassler type coreholder made of carbonfibre with polycarbonate end pieces. A net confining pressure of 20 bar was applied. The production of the displaced fluid phase was measured by an ultrasonic separator.

The tomographic images were taken using a third generation X-ray CT-scanner. The principle of computer tomograhy and its applications are described elsewhere (Hove et al., 1987; Wellington and Vinegar, 1987).

The CT-scans were made in a longitudinal plane of view. Slice thickness was 8 mm corresponding to about 27% of the total bulk volume. An image processing system was applied to quantify properties as porosity, saturations (Withjack, 1988) and permeability to water.

To visualize the dynamics of fluids during a flood, a subtraction between each image and a base image taken immediately before start, was performed. These subtracted images illustrate only the change in content of water during flooding. In other cases the quantified saturations are depicted. In all the CT-images in figures 2-6 the direction of flow is from right to left.

Analysis Programme

An oil base mud was used as drilling fluid and the 1.5″ plug was drilled from a seal peel using saline water. The sample was preserved in saran, aluminum foil and wax. The following sequence of experiments was carried out:

1. Analyses on the near neutral sample 1 (Case 1).
After core cleaning (solvents) the sample was saturated with chloride water. A miscible displacement and succeeding drainage and imbibition tests at different rates were CT-visualized. Hg-injection, thin section and SEM analyses were done on an end cap.
2. Analyses on sample 1A. Imbibition from low S_{wi} (Case 2).
After core cleaning the sample was saturated with iodide water and drained with oil using the centrifuge technique. A waterflood at low rate and increased rate in steps was then visualized.
3. Analyses on sample 1A. Imbibition from high S_{wi} (Case 3).
As case 2, but S_{wi} was established in an oilflood at 400 ml/h.
4. Analyses on the fired sample 1B (Case 4).
As case 3, but the sample was also fired at 600 °C to have a water wet reference to the previous displacement tests. Thin section and SEM analyses were carried out to study changes in porestructure.

RESULTS

The experimental results are presented under the following headings (1) Miscible displacement; (2) Oil- and waterfloods.

Miscible Displacement

A stable unit mobility displacement of chloride- by iodidewater was performed on sample 1 at rate 60 ml/h and is depicted in figure 2. A large channeling effect is observed. Water flows through a more permeable zone in the middle of the plug before the other zones of the sample are swept. The small differences in densities and viscosities did not cause gravity segregation nor viscous fingering.

The permeability to water, K_w, in the different layers of the sample is estimated using the equation

$$K = \frac{Q}{A} \cdot \mu \cdot \frac{L}{\Delta p} = \phi \cdot \frac{\Delta x}{\Delta t} \cdot \mu \cdot \frac{L}{\Delta p}$$

where

$$\phi \bullet \frac{\Delta x}{\Delta t} = \phi \bullet \frac{Q}{A\phi}$$

The 50% iodide/50% chloride concentration is chosen as the "tracer" to read the distance (Δx) the front moves during a certain period of time (Δt). Further, the average porosity for the sample is used since the variation in the actual porosity is relatively small. Applying this technique, K_w of about 2700 mD in the middle zone of the plug is estimated. In the upper and lower zones it is estimated to appr. 900 mD. Assuming that the middle zone represents half of the sample, an aritmetical mean of 1800 mD is calculated. Thin section analyses and corephotos confirm this laminated structure qualitatively.

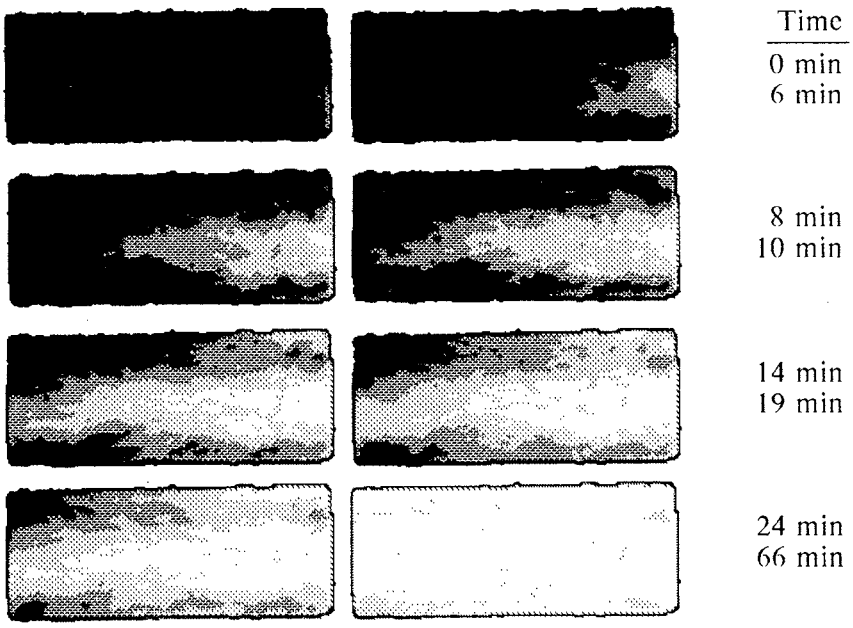

FIGURE 2 Miscible displacement of chloride water by iodide water, at 60 ml/h for 21 hours. The scale is increasing concentration of iodide water; 0.0 (black) to 1.0 (white).

Oil- and Waterfloods

The oilfloods at 400 ml/h lasted for about 24 hours, including 2-4 hours flooding with viscous oil in some experiments. Low and high rate waterfloods which lasted for minimium 24 hours and for about 10 hours respectively, are visualized. The main results obtained in these displacement tests are summarized in appendix, which generally indicate a good agreement between material balance- (MB) and CT-data. Only when the viscous oil was used, a few data in case 1 had to be corrected according to the quantified CT-images. In case 4 there is no explanation for the discrepancy between the saturation values.

Case 1: Tomography studies on sample 1

The primary drainage (oilflood at 400 ml/h) is depicted in figure 3. The oil first floods through the middle zone of the sample, similar to the miscible flood. Hence, the displacement of water is not very effective, and a high average $S_{wi} = 0.4$ is established. In some regions, especially in the lower part of the plug, S_{wi} is even higher than 0.75 after the production of water ceased. No significant production of water was registered neither during the following viscous oil flood nor during the displacement of viscous oil by a low viscosity oil. An emulsion was created at the interface between oil and water in the separator, giving rise to uncertainties in estimation of S_{wi}. However, according to the CT-images there is a significant change in water saturation before and after the flood with viscous oil. Especially there is a change near the outlet. The distribution of water becomes very non-uniform in the sample.

The largest recovery in the succeeding waterflood at 4 ml/h was obtained in the more permeable zone initially containing a higher oil saturation. For the lower permeability zones, almost no oil is displaced in this waterflood. According to the material balance there is a larger change in saturation than indicated on the images when the rate was increased from 40 to 400 ml/h. Production from the non-visualized parts of the sample can contribute to this additional oil production.

The channeling effect was observed in the following secondary drainage at 400 ml/h, as in the primary drainage. Almost no water was displaced from the lower permeable zones during this low viscosity oilflood.

Subtracted CT-images from a succeeding waterflood at medium rate 40 ml/h are shown in figure 4. Again water is flowing mainly in the higher permeable zone. Some more oil is mobilized from the

upper zone compared to the flood at 4 ml/h increased to 40 ml/h. This can explain the higher K_w (S_{or}) for this 40 ml/h case.

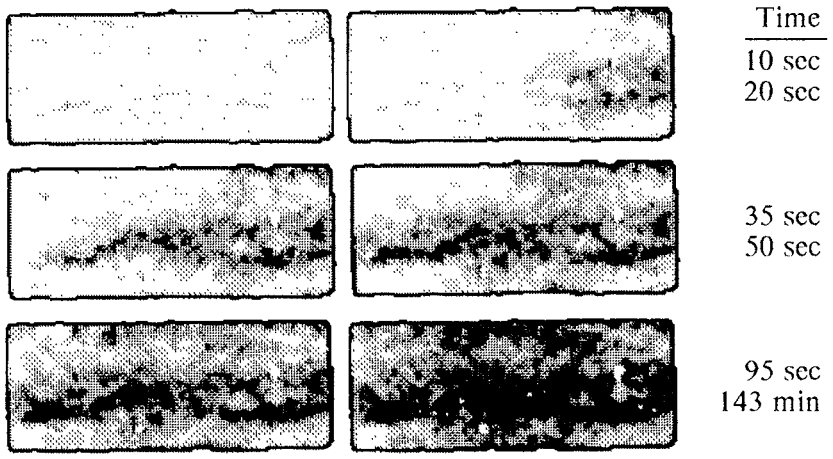

FIGURE 3 Primary drainage of sample 1 at 400 ml/h. The saturation scale, S_w is decreasing from white to black.

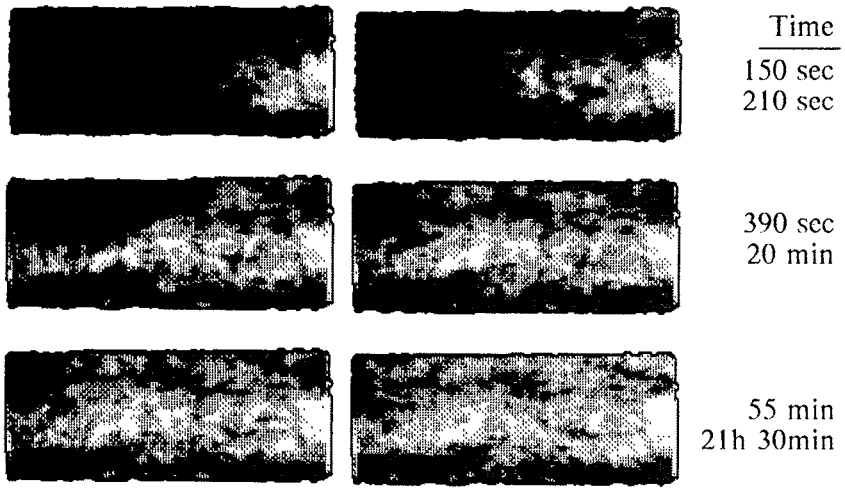

FIGURE 4 Waterflood on sample 1 at 40 ml/h (subtracted images). The lightest colour indicates the injected water.

An oilflood carried out at 400 ml/h is almost identical to the previous secondary drainage. Low viscosity and viscous oil were used.

The final high rate waterflood at 400 ml/h on sample 1 shows a channeling effect, even more pronounced than in the previous floods. But the recovery of the oil in the upper part of the sample seems to be higher than in the waterflood with rate 40 ml/h. A relative permeability curve for this waterflood is calculated, using the JBN-method (Johnson et al., 1959), and will be commented later.

Case 2: Study of the waterflood from a low S_{wi} on sample 1A.

After case 1 the corelength was reduced to fit the centrifuge equipment. The sample was cleaned and an oil/water capillary pressure curve was measured. A CT-image indicated that the distribution of the established S_{wi} = 0.13 was relatively uniform. A strong channeling effect as in case 1, occurs in the succeeding low rate waterflood (4 ml/h), with rate increased in steps to 170 and 400 ml/h. Again a high S_{or} was established.

Case 3: Study of waterflood from a high S_{wi} on sample 1A

After case 2 the sample was again cleaned with solvents and new displacement tests were performed.

The primary drainage at rate 400 ml/h is depicted in figure 5. The channeling effect is as described for the longer sample 1. The high water saturation near the outlet (end effect) decreases the measured $K_o(S_{wi})$.

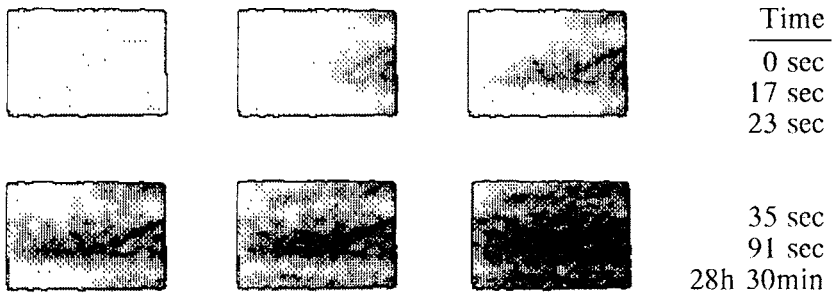

FIGURE 5 Primary drainage of sample 1A at 400 ml/h. The water is represented by the lightest colour.

The succeeding displacement of oil at 4 ml/h is different from what was observed in case 2. The imbibition starts very late in the middle part of the sample where S_{wi} is lowest. There is no detectable change in the images from the end of the waterflood at 4 ml/h and after increased rate to 170 ml/h and to 400 ml/h respectively.

Case 4: Water- and oilfloods on the fired sample 1B

Sample 1A was cleaned with solvents and fired to have a waterwet reference (renamed to 1B).

CT-images of primary drainage at rate 400 ml/h are presented in figure 6. Water in the lower part of the sample is drained first, and the water saturation becomes lower here than in the other parts of the sample. A smaller zone in the upper part near the outlet stays at a very high water saturation, even after continuous flooding with viscous and low viscosity oil for 28 hours.

In the subsequent waterflood at 4 ml/h, the images show that the displacement starts with a good distribution at the inlet. Because of the high content of water in the upper zone, the greatest change in water saturation occurs in the lower zone.

A less pronounced channeling effect is observed in this flood also after increasing the rate in steps to 170 and 400 ml/h. Stronger capillary forces might prevent fingering. This may verify that the sample became more water wet after firing. The S_{or} is more uniformly distributed and lower than in any of the previous cases.

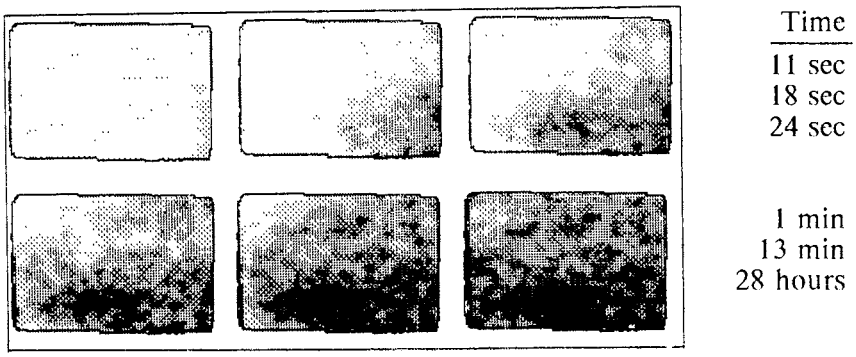

FIGURE 6 Primary drainage of sample 1B at 400 ml/h. The water is represented by the lightest colour.

DISCUSSION

Initial Water Saturation

The average initial water saturations obtained depend on the techniques used, see appendix. Some examples are:

(i) High speed centrifuge at $P_c \geq 2$ bar : $S_{wi} = 0.13$
(ii) Viscous oil flood at ≤ 400 ml/h : $S_{wi} \simeq 0.40$
(iii) Low viscosity oil flood at 400 ml/h : $S_{wi} \simeq 0.50$

A strong contributor to this is the variation of permeability in layers parallel to the direction of flow. The flow rate of oil in the lower permeability zones is reduced and prevents a strong reduction in S_w. In addition, the corresponding $K_o(S_{wi})$ will be suppressed by the higher water saturation.

The driving force in the centrifuge measurement is the strong gravity. The permeability variations in the sample is believed to have minor or no influence on the result of the drainage. The capillary pressure measurement has to be compared to the data corresponding to the height over free water level in the reservoir, in order to establish a representative S_{wi}.

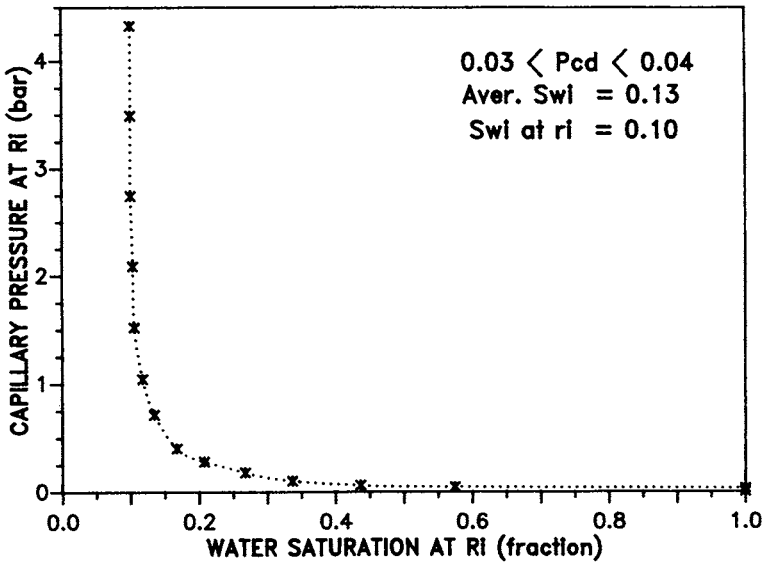

FIGURE 7 Oil/water capillary pressure curve (sample 1A) measured using the centrifuge technique (Hassler & Brunner, 1945).

A viscous-to-capillary force ratio (Fassihi, 1989) was applied to verify the high S_{wi} achieved in the oil floods. Some rough estimates were made, using the measured capillary pressure curve for oil/water drainage in figure 7 and some assumptions concerning the relative permeability data (Corey curve). The results indicate that a reasonable S_{wi} after flood with low viscosity oil is about 0.45, which is in good agreement with the measurements of S_{wi} . For lower water saturations the capillary forces are dominating. Since high flowrate were used, the only practical method to further reduce S_{wi} in a flood, is to increase the viscosity of the oil.

Recovery

The residual oil saturation is about 0.30 before firing this heterogeneous and near neutral sample. The S_{or} -level is only slightly reduced as the flowrate is increased. S_{or} seems to be independent on S_{wi} in the S_{wi}-range of these tests. After firing S_{or} becomes lower, probably due to a better vertical sweep during the flood.

The relative permeability endpoint to water, K_{rw} (S_{or}), is estimated using $K_o(S_{wi})$ prior to each of the waterfloods as a base. In general $K_{rw}(S_{or})$ is higher for lower S_{wi}. I.e. K_{rw} (S_{or}) increases with increasing change in water saturation during the waterflood (S_{or} is near constant) in case 1- 3. A contributor to this can be various distribution of fluids which cause different $K_w(S_{or})$ at a "fixed" S_{or} -level.

A comparison of the waterfloods from low and high S_{wi} in case 2 and 3 is done. The S_{wi} (0.13) in the centrifuge measurement is much lower and more uniformly distributed than the S_{wi} ($\simeq$0.5) achieved by flooding with oil. K_w (S_{or}) at 170 and 400 ml/h in case 2 is much higher than in the other cases, and it seems to be a function of the large change in water saturation during the waterflood. $K_o(S_{wi})$ is also higher in case 2 because of the low S_{wi}.

Effect of Flowrate and Core Length

The sample was cut at both endfaces to fit the centrifuge equipment. Hence some significant heterogeneities were removed. This change in plug size had an effect in some of the measurements.

The effective permeability to water, K_w, is increased from about 1750 to 2500 mD after reducing the length of the sample. This can be due to the removed parts of the sample and the additional core cleaning.

The S_{wi} and the corresponding $K_o(S_{wi})$ measured at high rate in case 1 are both lower than in case 3. The increase in S_{wi} -value as the core length was reduced can be due to more significant capillary end effect, resulting in higher S_{wi} near the outlet as stated in the litera-

ture (Rapoport and Leas, 1953). This should result in a lower $K_o(S_{wi})$ for case 3, but the opposite was measured. Since $K_o(S_{wi})$ is increased for the shorter sample, the removal of the heterogenieties influence the oil permeability more than increased capillary end-effects.

The increase in water saturation from S_{wi} during the low rate waterfloods were about 0.2 in all cases. The corresponding $K_w(S_{or})$ are less than 100 mD in cases 2 - 4, which is lower than for the longer sample in case 1.

A small change in water saturation was obtained when the rate was increased from 4 to 400 ml/h, except in case 2, were the S_{or} is significantly reduced. In all cases $K_w(S_{or})$ increased considerably. Generally during low rate floods there is time to distribute water outside the high permeability layer because of dispersion effects. A more severe fingering is observed early in this zone during the direct high rate waterflood.

S_{or} and K_w (S_{or}) in case 1 are almost the same after the direct high rate flood and after the test including increased rate in steps. This is probably due to the flow pattern of oil in the sample.

Relative Permeability Curve

The oil/water relative permeability curve for sample 1 in the high rate waterflood is calculated using the JBN-method and plotted in figure 8. Due to the high rate, we assume that the influence of the capillary forces are negligible. The strong channeling effect gives an early breakthrough of water. Hence, two phase production starts earlier and at a lower differential pressure than expected for a homogeneous sample with the same average permeability. After breakthrough the pressure drop starts decreasing slowly, and a close to linear appearance of the K_{rw} curve is achieved.

This example indicates that although S_{or} is only slightly dependent on the flowrate, alternative techniques to the JBN-method for determining relative permeabilities should be applied for heterogeneous samples. The procedure has to include capillary pressure and heterogeneities, and use of a visualization technique will be very important. Numerical simulation is also recommended.

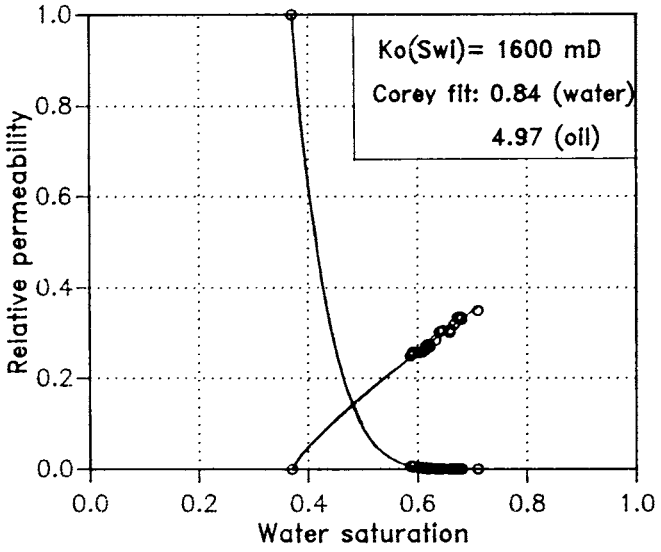

FIGURE 8 Imbibition curve at rate 400 ml/h for sample 1.

Effect of Firing the Sample

SEM analyses and CT-quantification of water and oil floods indicate a change in pore structure, porosity distribution and flood behaviour after the sample was fired. The SEM analyses show a small change in kaolinite from being dominantly presented as "booklets" in sample 1 to generally more "blocky" in sample 1B. Concerning illite, a fibrous morphology of this clay mineral is commonly observed in sample 1 but is not present in 1B. This change in clay structure might influence the macroporosity.

The imbibition process is more pistonlike than in the previous cases studied, and the differential pressure during the waterflood indicates lower permeability to water. A wettability test (Amott, 1958) performed on sample 1B gave indices for water and oil of 0.9 and 0.0 respectively, characterizing the sample as strongly waterwet. $K_{rw}(S_{or})$ is also reduced from about 0.4 to 0.1. S_{wi} is increased and S_{or} is slightly decreased.

Figure 9 compares the distribution of water at the end of the floods before and after firing. Two "layers" with different S_{wi} are observed in the fired sample. S_{or} is lower and more uniformly distributed after firing. No significant change in saturation distribution is observed between 170 and 400 ml/h end points.

The middle layer of the sample is more porous after firing. The estimated average porosities from the CT-images of sample 1A and 1B are 18.0 and 20.5% respectively. The width of the porosity distribution is about the same for both samples.

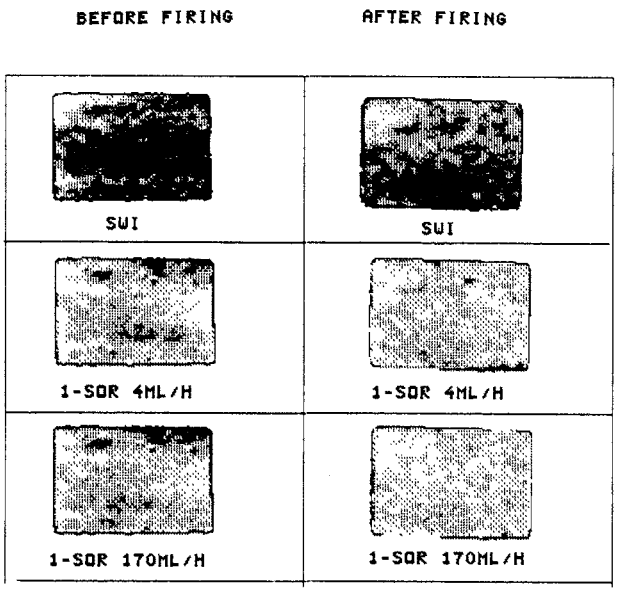

FIGURE 9 Saturation distribution at S_{wi} and S_{or} before (1A) and after (1B) firing (black indicates lowest water saturation).

CONCLUSIONS

1. Tomograhic visualization of miscible displacement in a porous medium is an excellent method to describe the sample, and gives valuable information to interpret data from immiscible displacements.
2. The CT-images confirm that the layers with different permeability and porosity have a pronounced effect on the production history in the high rate imbibition tests. Tomograhy should therefore be used to select as homogeneous samples as possible for special core analyses.
3. Using traditional methods to calculate relative permeability curves on strongly layered samples should be avoided. Displacement

endpoints can be determined, but tomographic visualization might be necessary.
4. The established level of initial water saturation is dependent on the technique used in the laboratory. It should be compared to the S_{wi} -value recommended according to the height over free water level in the reservoir and the corresponding capillary pressure curve. The centrifuge technique is preferred to establish S_{wi} when the oil column is thick.
5. The effect of flowrate on S_{or} for this near neutral, and heterogeneous sample is not pronouced. The layered structure in the sample contributes to the relatively high residual oil saturation also obtained at high flowrates. The S_{or} seems to be independent on S_{wi}.
6. $K_w(S_{or})$ appears to be a function of change in water saturation during the waterfloods.
7. The sample became water wet after firing, but a change in the clay structure also occured. Hence, firing of cores should not be used uncritically to obtain water wet samples.

ACKNOWLEDGEMENTS

The authors would like to thank Magne Skarestad and Jon K. Ringen for advices and comments to the manuscript. We are also grateful to colleagues at the Geological Laboratory, Statoil, for performing thinsections and SEM analyses.

NOMENCLATURE

A	:	cross sectional area of the sample (m^2)
$K_o(S_{wi})$	:	permeability to oil at S_{wi} (mD)
$K_w(S_{or})$	:	permeability to water at S_{or} (mD)
L	:	sample length (m)
Q	:	injection rate (m^3/s)
Q/A	:	Darcy velocity (m/s)
S_{or}	:	residual oil saturation (fraction)
S_{wi}	:	initial water saturation (fraction)
Δp	:	pressure difference inlet to outlet (Pa)
μ	:	viscosity (mPas)
ϕ	:	porosity

REFERENCES

AMOTT, E. (1958). Observations relating to the wettability of porous rock. *Trans., AIME*, **216**, 156-162.

FASSIHI, M.R. (1989). Estimation of relative permeability from low rate, unsteady-state tests -A simulation approach. *Journal of Canadian Petrolum Technology*, **28**, 29-38.

HASSLER, G. L. and BRUNNER, E. (1945). Measurement of capillary pressures in small core samples. *Trans., AIME.*, **160**, 114-123.

HOVE, A., RINGEN, J.K. and READ, P.A. (1987). Visualization of laboratory corefloods with the aid of computerized tomography of X-rays. *SPE Res. Eng.*, **2**, No. 2, 148-154.

JOHNSON, E.F., BOSSLER, D.P. and NAUMANN, V.O. (1959). Calculation of relative permeability from displacement tests. *Petroleum transactions, AIME*, **216**, 370-372.

RAPOPORT, L. A. and LEAS, W. J. (1953). Properties of Linear Waterfloods. *Trans. AIME*, **198**, 139-148.

WELLINGTON, S.L. and VINEGAR, H. J. (1987). X-ray computerized tomography. *Journal of Petr. Techn.*, **39**, 885-898.

WITHJACK, E. M. (1988). Computed tomography for rock-property determination and fluid-flow visualization. *SPE Formation Evaluation*, **3**, no 4., 696-704.

APPENDIX

Main results from the tomography cases 1-4

Case	*Rate (ml/h)*	S_{wi} *(MB)*	S_{wi} *(CT)*	S_{or} *(MB)*	S_{or} *(CT)*	$K_o(S_{wi})$ *(mD)*	$K_w(S_{or})$ *(mD)*
1	q_o = 400	0.45	0.47	-	-	1272	-
	q_o = 400[a]	0.40	0.40	-	-	1366	-
	q_w = 4	-	-	0.35	0.37	-	115
	q_w = 40	-	-	0.32	0.34	-	369
	q_w = 400	-	-	0.27	0.33	-	580
	q_o = 400	0.43	0.43	-	-	1317	-
	q_w = 40	-	-	0.36	0.34	-	462
	q_o = 400	0.37	0.39	-	-	1272	-
	q_o = 400[a]	0.35	0.37	-	-	1600	-
	q_w = 400	-	-	0.29	0.35	-	560
2	centrifuge	0.129	0.135	-	-	2443	-
	q_w = 4	-	-	0.71	0.73	-	64
	q_w = 170	-	-	0.39	0.42[b]	-	1084
	q_w = 400	-	-	0.32	-	-	1458
3	q_o = 400	0.51	0.51	-	-	1585	-
	q_o = 400[a]	0.49	0.43	-	-	2032	-
	q_w = 4	-	-	0.34	0.35	-	98
	q_w = 170	-	-	0.33	0.34	-	467
	q_w = 400	-	-	0.30	0.33	-	592
4	q_o = 400	0.64	0.55	-	-	2229	-
	q_o = 400[a]	0.59	0.48	-	-	3725	-
	q_w = 4	-	-	0.26	0.29	-	81
	q_w = 170	-	-	0.20	0.28	-	292
	q_w = 400	-	-	0.18	0.26	-	391

[a] After flood with viscous oil.
[b] After 44 minutes, not at equilibrium.

S_{wi} (MB) : Initial water saturation from material balance.
S_{wi} (CT) : Initial water saturation from tomography.
S_{or}(MB) : Residual oil saturation from materialbalance.
S_{or}(CT) : Residual oil saturation from tomography.
$K_o(S_{wi})$: Permeability to oil at S_{wi}.
$K_w(S_{or})$: Permeability to water at S_{or}.

Case 1: Analyses on the near neutral sample 1 before reduction of the core length.
Case 2: Analyses on sample 1A. Imbibition from low S_{wi}.
Case 3: Analyses on sample 1A. Imbibition from high S_{wi}.
Case 4: Analyses on the strongly water wet fired sample 1B.